New developments for the use of microphysical variables for the assimilation of IASI radiances in convective scale models

P.Martinet[1], N.Fourrié[1], F.Rabier[1], V.Guidard[1] ,T.Montmerle[1], P.Brunel[2], L.Lavanant[2]

[1]Météo France & CNRS/CNRM-GAME, Toulouse, France
[2]Météo France, Centre de Météorologie Spatiale, Lannion, France

ABSTRACT

This paper focuses on the simulation and the assimilation of IASI (Infrared Atmospheric Sounding Interferometer) observations in convective scale numerical weather prediction (NWP) systems. A radiative transfer model that includes profiles for liquid water content, ice water content and cloud fraction was used to simulate cloud-affected radiances as background equivalents. This approach avoids the use of cloud parameters (cloud top pressure and effective cloud fraction) deduced from a CO2 slicing algorithm and the modelling of clouds by single layer clouds. The observation-screening procedure that was developed to improve the selection of usable cloudy scenes led to a good agreement between observations and background equivalents. For that purpose, a radiance analysis of co-located AVHRR (Advanced Very High Resolution Radiometer) pixels inside each IASI field of view was used. The goal of this preliminary work is to assess the feasibility of adding the cloud variables (liquid and ice water contents) to the state vector of the assimilation system. As it is not feasible to assimilate all the 8461 channels of IASI, we decided to evaluate the capability of the 366 channels (Collard and McNally 2009) used operationally at the European Centre for Medium-Range Weather Forecasts (ECMWF) on cloud profiles. To this selection (called CM2009 hereafter), 134 new channels were added to optimize the retrieval of microphysical variables focussing mainly on the Mediterranean Sea. A linear approach based on the Degrees of Freedom for Signal (DFS) was compared to a non-linear method based on the brightness temperature response to the perturbation of cloud variables. To validate the new selections, observing system simulation experiments (OSSE) were used in the context of one-dimensional variational (1D-Var) retrievals.

INTRODUCTION

Nowadays, satellite observations are an important source of data assimilated in numerical weather prediction (NWP) models. They contribute positively to NWP analysis and the accuracy of forecasts (Kelly and Thépaut 2007).

The Infrared Atmospheric Sounding Interferometer (IASI) on-board the MetOp satellite belongs to a new generation of advanced infrared sounders and follows the launch of the Atmospheric InfraRed Sounder (AIRS) on-board the Aqua satellite in 2002. AIRS with 2378 channels and IASI with 8461 channels provide information about atmospheric temperature and humidity with a far better spectral resolution compared to previous instruments such as the High Resolution InfraRed Sounder (HIRS).

All the NWP centres intend to increase the number of assimilated satellite observations which are limited, most of the time, to clear-sky locations. For instance, only 3% of the screened radiances are used in the operational data assimilation at the European Centre for Medium-Range Weather Forecast (ECMWF) according to Kelly and Thépaut (2007). This under-exploitation of satellite data is partly caused by a rejection of cloud-affected radiances during the assimilation process because of large innovations (observation minus background) due to cloud mislocation or deficiencies in the modelling of clouds, either in radiative transfer (RT) models or NWP models. The high correlation between cloud cover and meteorologically sensitive areas underlines the need to use infrared observations in presence of clouds (McNally 2002, Fourrié and Rabier 2004).

Nevertheless, an incorrect modelling of clouds leads to increased errors in the RT calculations especially in the infrared (IR) spectral range which is very sensitive to cloud microphysical properties. Different techniques have been developed in the frame of global models to overcome this problem. Most of them (Pavelin et al 2008, McNally 2009, Pangaud et al 2009) are based on the use of two cloud parameters, the cloud top pressure (CTOP) and the effective cloud fraction (Ne) to directly assimilate cloud-affected radiances. However, these techniques use a simplified modelling of clouds assuming single layers of opaque clouds and the calculationof the CTOP and Ne can be problematic in the case of low clouds or thin high clouds.

In this study, we propose new developments for the assimilation of cloud-affected radiances taking advantage of the high resolution of convective scale NWP models. Their kilometre-size grid mesh,

non-hydrostatic equations and microphysics parametrizations enable a better modelling of cloud variables such as liquid water content (ql), ice water content (qi) and cloud fraction.
The main purpose of this paper is to assess the feasibility of adding cloud profiles (ql,qi) in the control vector of a 1D-Var assimilation system preparing for the direct assimilation of such profiles in the three-dimensional variational data assimilation (3D-Var) system of the French operational AROME model (Seity et al 2011).
To prepare the 1D-Var, an observation-screening procedure permitting an improved selection of homogeneously covered scenes from IASI observations was developed. The feasibility of using cloudy fields from mesoscale NWP models to simulate cloudy radiances was investigated. To that end, the fast RT model RTTOV has been used to improve the simulation of multi layer clouds. We evaluated the simulated cloud-affected radiances and their departures from observations.
In order to optimize the retrievals of microphysical variables, new channels were added to the 366 IASI channels selected by Collard and McNally 2009 (called CM2009 selection hereafter).
Finally, some 1D-Var experiments using Observing System Simulation Experiments (OSSE) are presented.

EXPERIMENTAL FRAMEWORK

In order to convert atmospheric profiles from the NWP model into simulated radiances, the fast radiative transfer model RTTOV is used. The version 10.1 of RTTOV (Hocking et al 2010) used in this study contains an advanced interface to include ql, qi and cloud fraction profiles called RTTOVCLD hereafter. The advanced interface RTTOVCLD enables a better modelling of clouds with the possibility of multi-layer clouds and two cloud types per layer. Absorption is computed in each of the 101 fixed vertical levels from the interpolated cloudy profiles using fast transmittance coefficients calculated by the line-by-line transmittance model LBLRTM.
The convective scale model AROME (Application of Research to Operations at MEsoscale) with a 2.5 km grid mesh is used to provide cloudy profiles over the Mediterranean Sea during a period of 30 days (7 October 2010 to 7 November 2010).

THE AVHRR cluster

The Advanced Very High Resolution Radiometer (AVHRR) on MetOp is helpful to define the scene type (partially cloudy or overcast) and can also be used to select homogeneously covered cloudy scenes.
The AVHRR cluster provided by EUMETSAT in the IASI level1c files (Cayla 2001) proved to be a valuable tool. This product is based on a radiance analysis of co-located AVHRR pixels inside each IASI field of view (FOV). AVHRR measures the radiance emitted by the Earth in six spectral bands: two in the visible and four in the IR. All AVHRR pixels are aggregated in classes characterized by homogeneous properties in the radiance space using a K-means clustering. For each AVHRR class and each channel, the cluster product provides the mean radiance, the standard deviation and the coverage of the class within the IASI pixel. As the aggregation was performed with all the available AVHRR channels, the algorithm can produce several classes even with relatively small standard deviations for the IR channel. As a result, a FOV with several classes with each one a small standard deviation and a mean radiance close to that of the other classes can be more homogeneous than a FOV with a single class. This is the reason why the number of AVHRR classes inside each IASI pixel was not used as the homogeneity criterion. Alternatively, these characteristics were used to compute global statistics of the AVHRR cluster aggregating the information provided by all the classes within the IASI FOV. We focused on one of the IR channels (11.5 μm) to get closer to the scene observed by IASI.
We calculated a weighted average considering each mean radiance and standard deviation for the 11.5 μm band (weight depending on the coverage of the class within the IASI pixel). One part of the homogeneity criterion is based on the relative standard deviation calculated from these global statistics and represents the intra-class homogeneity of the AVHRR cluster. This first criterion assures that each AVHRR class is homogeneous but not that all the classes observe the same cloudy scenes. To evaluate the inter-class homogeneity, the standard deviation of the mean radiances of all the classes has been calculated.
The AVHRR cluster gives information about the scene observed by IASI but none about AROME. To keep scenes for which both the observation and the simulated radiance are homogeneous, the model homogeneity has been evaluated by a comparable method.
Similar statistics as the ones used from the AVHRR cluster are reproduced. We used each AROME grid point within the IASI spot to simulate the radiances measured in the 11.5 μm band by the AVHRR imager with the use of the radiative transfer model RTTOVCLD. The standard deviation between each

simulated radiance is the equivalent in the model space of the inter-class homogeneity and can be used to evaluate the model homogeneity (Martinet et al 2012). The concepts of inter-class and intra-class homogeneity in the model space and the observation space were used to select homogeneously covered cloudy scenes.

The relative standard deviation from the AVHRR cluster is correlated with the homogeneity of the scene. Our study is performed over a period of 30 days (7 October 2010 to 7 November 2010) on a domain centred on the Mediterranean Sea.

A scatterplot comparing the values of effective cloud fraction (on the abscissa) and cluster relative standard deviations is given in Figure 1. The top left panel represents the inter-class homogeneity of the observed cluster, the top right panel represents the equivalent of this criterion in the model space. The bottom panel shows the intra-class homogeneity of the observed cluster. The values of effective cloud fraction were computed by a CO2 slicing algorithm on a IASI spectrum for the observed cluster and an AROME simulation for the simulated cluster.

These plots give a calibration of what a low standard deviation is (homogeneous scene) and what a high value is (heterogeneous scene) in order to set a threshold. The thresholds used for the definition of homogeneous scenes must lead to a sufficient size of the selected dataset and avoid the selection of fractional clouds. We decided to select an observation if it fulfils the three criteria:

- Intra-class homogeneity of the observed cluster < 4% (weighted average of the standard deviations of each class);
- Inter-class homogeneity of the observed cluster < 8% (standard deviation of the mean radiances of each class);
- Inter-class homogeneity of the simulated cluster < 8% (standard deviation of AVHRR simulations from each AROME grid point in the FOV.).

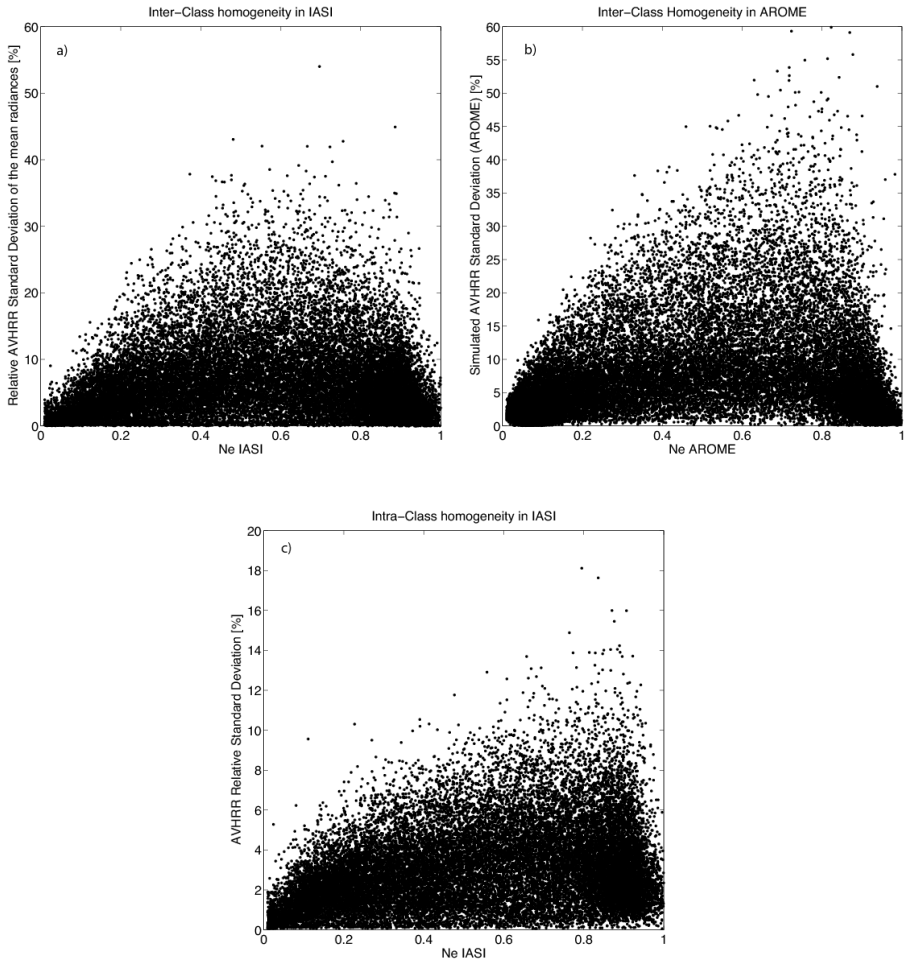

Figure 1: **Scatterplot comparing the values of effective cloud fraction (on the abscissa) and the cluster relative standard deviation (on the ordinate) (a) for the inter-class homogeneity of the observed AVHRR cluster (b) for the cluster simulated with AROME, (c) for the intra-class homogeneity of the observed AVHRR cluster.**

EVALUATION OF THE OBSERVATION OPERATOR

In this section, we monitor simulated and observed cloudy IASI radiances during our 30-day test period over the Mediterranean Sea.

To be assured that the monitoring focused on overcast scenes, the percentage of cloudy AVHRR pixels within the IASI FOV has been used in addition to the selection of homogeneous scenes previously described. IASI observations with 100% of cloudy AVHRR pixels were kept.

In this screening-procedure, we imposed the cloudiness of the observation by the amount of cloudy AVHRR pixels within the IASI FOV but we did not take into account the cloudiness of AROME. To sidestep this problem and check that both the observation and the model observe the same cloudy scene, we imposed that the difference between the mean AVHRR brightness temperatures from the observed and the simulated cluster is smaller than 7K. This new constraint is important to avoid a cloud mislocation between AROME and IASI and to be as close as possible to the true state.

Standard deviations and biases of the O-B (observation minus background) departures are shown in figure 2 for the different screenings: overcast scenes (left panel) and homogeneous overcast scenes with a condition on the AROME cloudiness (right panel). As should be expected, the best model statistics are found in channels least affected by clouds (CO2 and water vapour bands). Standard deviations are larger for window channels revealing a dependence on the vertical position of the sensitivity functions. Biases and standard deviations are large for overcast scenes (-7K and 20K respectively for window channels). Avoiding the cloud mislocation between AROME and IASI and focussing on homogeneously covered scenes significantly improves the bias (-1K for window channels). The standard deviation is also decreased by more than 10K to values less than 5K which is a considerable improvement.

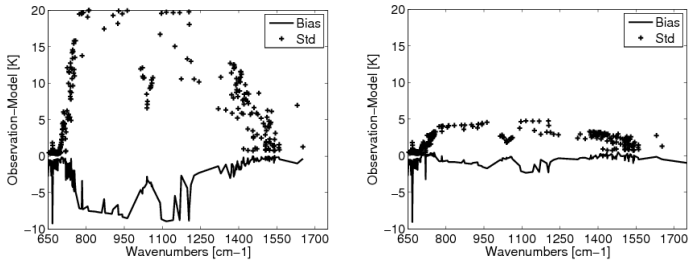

Figure 2: **Bias and standard deviation (Std) of the differences between the model and the cloud-affected observed IASI brightness temperatures over a 30 day period from 7 October 2010 to 7 November 2010 on the Mediterranean Sea. Left panel: considering all overcast observations, right panel: only homogeneous overcast scenes with a constraint on the AVHRR brightness temperature.**

These results prove some capability of the observation operator to simulate overcast scenes. The selection of homogeneous scenes with a constraint on the mean AVHRR brightness temperature enables to decrease the bias to a value more acceptable for the assimilation.

Before performing 1D-Var retrievals of microphysical variables, we decided to revise the already existing IASI channel selection to optimize the cloudy assimilations in the next sections.

CHANNEL SELECTION BASED ON THE DEGREES OF FREEDOM FOR SIGNAL (DFS)

The first channel selection that was chosen for this study is based on the methodology described by Rodgers (2000) which was shown to be the more optimal by Rabier et al 2002. The method consists in performing successive analyses considering only one channel at a time. The impact of the addition of single channels is evaluated by the DFS which is used as the figure of merit of the channel selection :

$$DFS=tr(\mathbf{I}-\mathbf{AB}^{-1})$$

where Tr denotes the trace, **I** the identity matrix, **A** is the analysis-error covariance matrix and **B** the background-error covariance.

The background-error covariance matrix **B** is updated at the next step by the analysis-error covariance matrix **A** previously calculated. In order to take into account the gain brought by the previously selected channels, this update of the **B** matrix is important.

The starting point of the study is the CM2009 (Collard and McNally 2009) selection composed of 366 IASI channels. Firstly, the analysis-error covariance matrix **A** considering the 366 IASI channels of the CM2009 selection is evaluated. Then, new channels are selected updating the **B** matrix by the previously calculated **A** matrix. The atmospheric components for which information is expected are temperature, humidity, liquid water content (ql) and ice water content (qi).

PHYSICALLY-BASED CHANNEL SELECTION

The second channel selection methodology was used by Gambacorta and Barnet 2011 for the Cross-Track Infrared Sounder (CrIS) and is called physical method hereafter. A spectral sensitivity study of the full IASI spectrum has been led with RTTOVCLD. We evaluated the brightness temperature (BT) response to the perturbation of each atmospheric constituent separately: ql, qi, temperature (T), skin temperature (Tskin), humidity (q), ozone (O_3), methane (CH_4), carbon monoxide (CO). The brightness temperature response ΔBT_v is represented by the difference between the RTTOVCLD simulation with the perturbed profile and the unperturbed profile. These BT differences indicate the sensitivity of each channel to each specific atmospheric species.

Figure 3 is an example of this sensitivity analysis applied on three profiles representative of semi-transparent ice cloud, ice opaque cloud and liquid cloud over the Mediterranean Sea. Each curve represents the difference in brightness temperature due to the perturbation of each one of the atmospheric species. We can notice that the sensitivity analysis is highly dependent on the cloudy profile. Based on the sensitivity analysis, channels with the highest sensitivity to ql and qi variables and the lowest sensitivity to the other species are chosen.

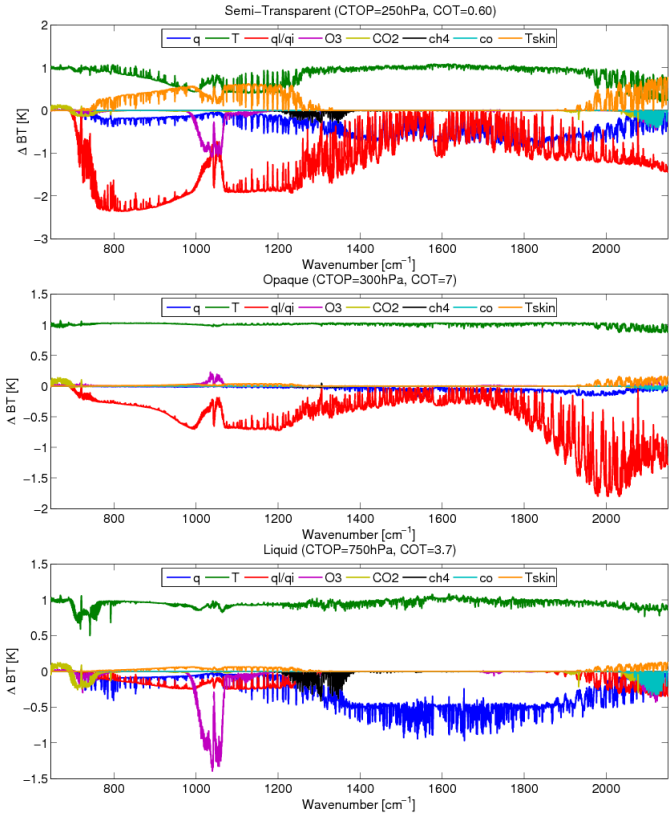

***Figure 3*: Sensitivity analysis of IASI channels. Blue curve: humidity perturbation. Green curve: temperature perturbation. Red curve: ql and qi perturbation. Cyan curve: CO. Dark purple: O_3.Orange curve: skin temperature. Light green: CO_2. Black curve: CH_4. The sensitivity analysis is performed for three cloud types: semi-transparent ice cloud(top), opaque ice cloud(middle) and liquid cloud (bottom). The cloud top pressure and the cloud optical thickness derived from the ql and qi profiles are given for each cloud type.**

COMPARISON OF SELECTED CHANNELS

Figure 4 shows the two global selections considering the DFS method or the physical method. The channels selected by ice opaque clouds are displayed in blue points, the ones selected by semi-transparent ice clouds in black points and the ones selected by liquid clouds in red points.

In the physically-based selection, water vapour channels are not chosen as we minimize the sensitivity of the spectrum with respect to humidity and the sensitivity of water vapour Jacobians.To discuss the results, four spectral regions were designed and correspond to those described in table1. Even if only 52 channels are shared by the two methods of selection, most of the channels are located in the window regions A and D of the IASI spectrum (650-1000 cm^{-1}, 1800-2150 cm^{-1}). In fact, in window regions the transmittance is close to one and the flux emitted by the surface can reach the satellite. In cloudy condition, the surface emission is partly or totally attenuated by the cloud and the upwelling information mainly comes from the cloud top pressure. The DFS selection favours the window

channels at the end of the water vapour band (D) whereas the channels selected with the physical approach are almost equally divided between the window regions A and D.

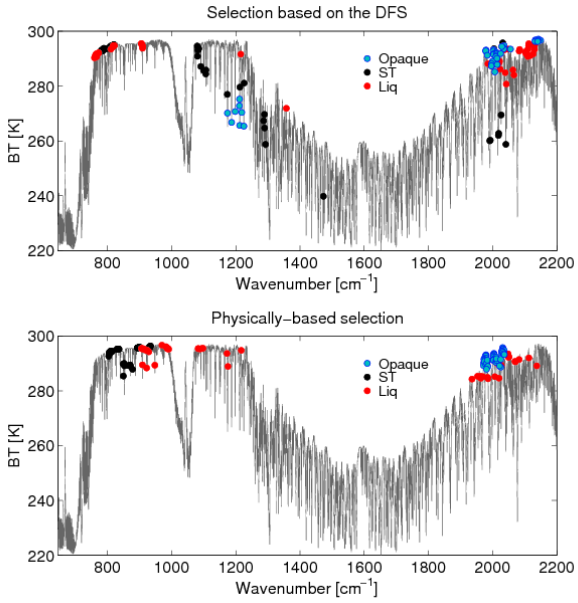

***Figure 4*: Location of the selected channels averaged over 15 representative profiles chosen for the selection. The DFS selection (top) is compared to the physical selection (bottom).**

Band	Wavenumber (cm^{-1})	DFS selection	Physical Selection
A	650-1000	36	61
B	1090-1200	13	6
C	1200-1800	14	1
D	1800-2150	71	66

***Table1*: Number of channels selected in different spectral regions of a typical IASI spectrum for both channel selections.**

We can note that wings of transition lines are most often selected by the DFS method (essentially in the water vapour band). In clear conditions, it was shown that selecting channels along the wings of transition lines, sharper weighting functions were obtained (Kaplan et al 1977). However, in cloudy conditions all the Jacobians of liquid water content and ice water content peak around the cloud top pressure and have almost no sensitivity to levels under or above the cloud top pressure. Thus, it would be useless to base our channel selection on the shape of the weighting functions. As we are interested in the addition of channels sensitive to cloud variables without any interference with other variables, channels in the wings of transition lines can also be too sensitive to water vapour.
Even if the two selections do not choose the same channels, they are located in the same spectral bands. Consequently, it is important to evaluate if the two selections are as suitable to use for cloudy retrievals.
As the main goal of this study is to optimize the 1D-Var retrievals of microphysical variables, each channel selection is validated with OSSE. The root-mean-square errors (RMSE) of the analysis performed by the 1D-Var against the `truth' is compared using the two channel selections in the next section.

EVALUATION OF THE TWO CHANNEL SELECTIONS

1D-Var retrievals in the context of OSSE

We have chosen to perform 1D-Var retrievals at this stage in order to test our channel set. As no observation is available to validate the retrievals, the 1D-Var is evaluated in the context of OSSE. For that purpose, the background profiles are generated from the AROME profile dataset perturbed with the addition of simulated forecast errors. The observations are generated from the `true' background profiles and simulated observation errors are added. 1D-Var retrievals are performed on a subset of 588 ice opaque clouds, 390 semi-transparent ice clouds and 240 low liquid clouds using the 1D-Var

code (version 3.3) provided by the Met Office in the framework of the EUMETSAT NWP Satellite Application Facility (Pavelin and Collard 2009). Cloud variables have been added to the state vector of the 1D-Var interface.
The two selections are compared between each other and the improvement brought to the CM2009 selection is shown in Figure 5.
Firstly, we can note that whatever the channel selection is, the profiles of RMSE indicate that the analyses are always better than the backgrounds for cloud variables demonstrating the robustness of the channel selection algorithm employed by Collard 2007 to provide the main part of the CM2009 selection. Indeed, in the CM2009 selection, even if only 20 channels were specifically added for surface emissivity and cloud variables, about 130 channels were selected in window regions because of temperature and humidity variables (most of them being located in band A).
Secondly, we can note that the new channel selections are better than the CM2009 selection for the analysis of ice water content for opaque clouds and liquid water content for low clouds. However, for semi-transparent clouds, the addition of 134 channels does not help improving the analysis of ice water content.

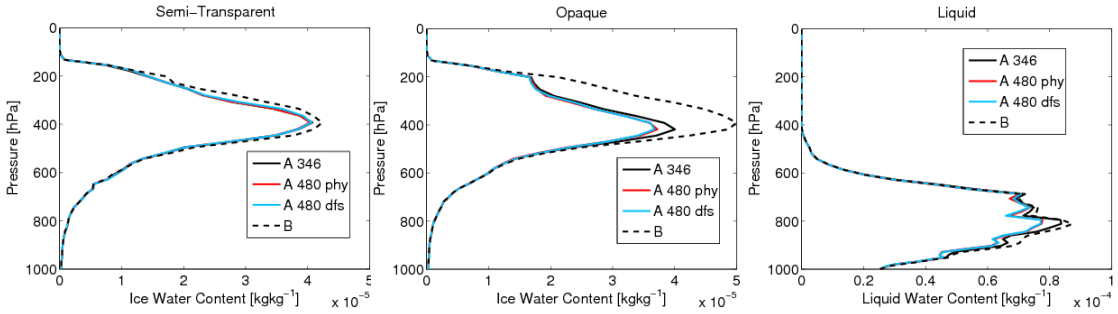

***Figure 5*: Vertical profiles of root-mean-square errors of the background and the analysis against the 'truth' (dotted and plain lines respectively) for ice water content of semi-transparent clouds (top panel), ice water content of opaque clouds (middle panel) and liquid water content of low clouds (bottom panel). Comparison between the analysis with the new channel selection based on the physical method (red line), the DFS method (blue line) and the CM2009 selection used operationally at ECMWF (black line)**

Finally, the analysis of cloud variables is equivalent when using the selection provided by either the DFS method or the physical method. This is an important result that confirms the relevance of the DFS even in non-linear cloudy retrievals. In fact, if the cloudy observations are well selected and the model profiles are close enough to the `true' state of the atmosphere, the approximation of the `true' state by a linear optimal estimation theory looks reasonable (Martinet et al 2012). In the context of the sounder AIRS and in clear conditions, Fourrié and Thépaut 2003 have also shown that the physically-based selection provides similar results in terms of analysis-errors to a global selection preserving the DFS.

Comparison of temperature and humidity Jacobians
As temperature, humidity and cloud variables are retrieved simultaneously, we need to make sure to remove the interference from other sources. Thus, a good way to evaluate the quality of the selection is to study the shape of temperature and humidity Jacobians for each channel selection (Figure 6). In Figure 6, it is clear that the channels selected by the physical approach are less sensitive to humidity and temperature according to the Jacobian shapes. This comparison shows the superiority of the physically-based channel selection that minimizes the interaction with interfering species like humidity.
As we previously described, the DFS method favours the channels located in the wings of water vapour transition lines explaining the high values of humidity Jacobians for this selection.

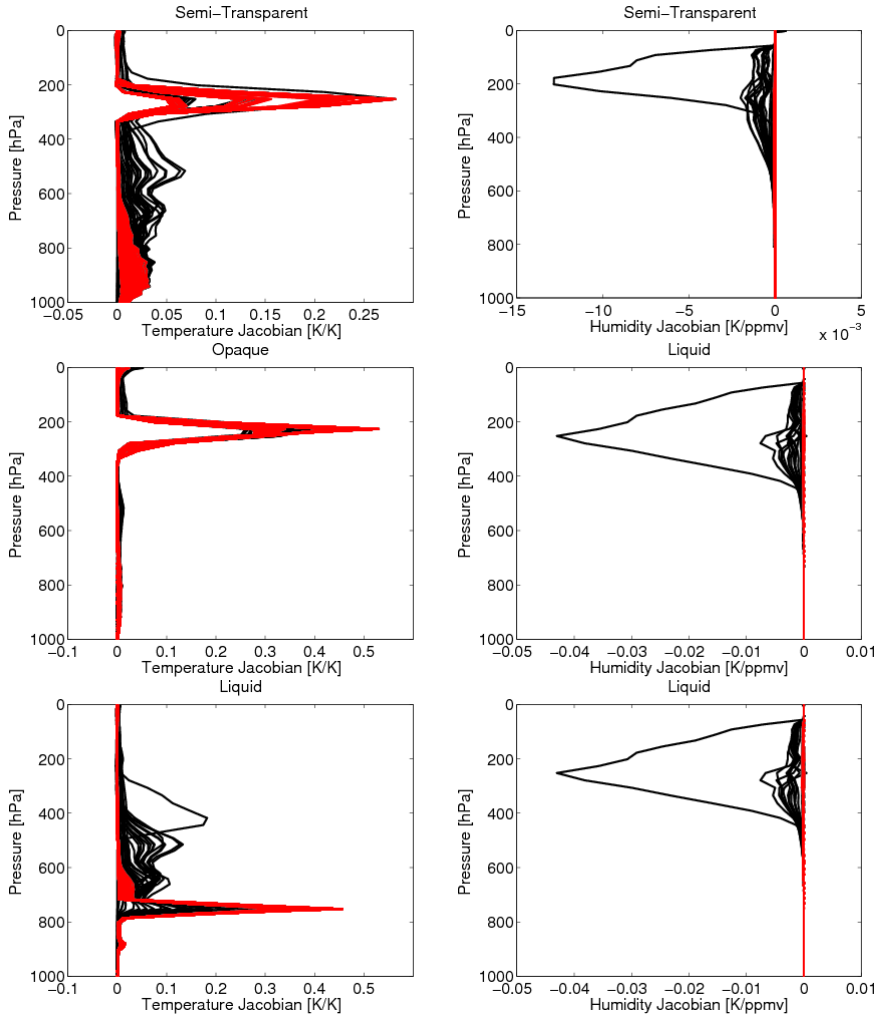

***Figure 6*: Temperature (left panels) and humidity (right panel) Jacobians for three representative cloud profiles: semi-transparent (top), opaque (middle) and liquid (bottom). The Jacobians are compared with the channels selected by the DFS method (black lines) or the physical approach (red lines).**

CONCLUSION

In this work, we have shown that encouraging results were obtained for the assimilation of IASI cloudy radiances using cloud microphysical variables.

Firstly, a screening procedure based on the AVHRR imager was shown to significantly improve the observation minus simulation innovations. Thus, the preselection of homogeneously covered scenes avoiding the cloud mislocation between the NWP model and the cloud-affected IASI observation is essential before any assimilation.

Secondly, the 366 IASI channels selected by ECMWF in clear conditions was evaluated for the retrieval of microphysical variables and 134 new channels were added to optimize the cloudy retrievals. For that purpose, two methods of selection were compared: the first one is a linear approach based on the DFS and the second one is a non-linear approach based on the brightness temperature response to the perturbation of cloud variables. Each selection was evaluated in terms of RMSE of 1D-Var retrievals using Observing System Simulation Experiments. It was shown that the ECMWF selection already provides good retrievals of liquid water content and ice water content. However, when deriving a specific channel selection on top of this one, a larger gain was obtained with both channel selections. The equivalence of the RMSE between the two channel selections confirms the quality of the selection based on the DFS which has already been implemented in other channel selections. Even if the observation operator used in this study is non-linear in cloudy conditions, the results of the DFS selection can be considered as reliable. However, it has been shown that the physically based approach provides sharper temperature Jacobians and a smaller sensitivity to water vapour compared to the DFS method. Minimizing the interference with atmospheric species like humidity, the physically based selection was found to be preferred over the DFS method. These revised IASI channel selections will be the subject of a dedicated publication.

In the future, we will evaluate the potential benefit of these microphysical variables in the NWP model AROME. As the inclusion of the cloud water contents in the state vector has not been implemented yet, a one dimensional version of AROME will be used for this study. An AROME forecast will be run on the analysed profiles to evaluate the capability of AROME to keep the cloud information provided by IASI during the first time steps of simulation.

References

- Cayla F-R, 2001. AVHRR Radiance Analysis inside IASI FOV's. IA-TN-0000-2092-CNE, *CNES internal report*.
- Collard A, 2007. Selection of IASI channels for use in numerical weather prediction. *Quart.J.Roy.Meteor.Soc*., **133**, 1977-1991.
- Collard A, McNally A.P, 2009. The assimilation of Infrared Atmospheric Sounding Interferometer radiances at ECMWF. *Quart.J.Roy.Meteor.Soc.*, **135**, 1044-1058.
- Fourrié N, Thépaut J.N, 2003. Evaluation of the AIRS near-real-time channel selection for application to numerical weather prediction. *Quart.J.Roy.Meteor.Soc* , **129**, 2425-2439.
- Fourrié N, Rabier F, 2004. Cloud characteristics and channel selection for IASI radiances in meteorologically sensitive areas. *Quart.J.Roy.Meteor.Soc*, **128**, 2551-2556.
- Hocking J, Rayer P, Saunders R, Matricardi M, Geer A, Brunel P, 2010. RTTOV v10 Users Guide.NWPSAF-MO-UD-023, EUMETSAT, Darmstadt, Germany.
- Gambacorta A, Barnet C, 2011. Methodology and Information Content of the NOAA/NESDIS Operational Channel Selection for the Cross-Track Infrared Sounder (CrIs). *NOAA Technical Report NESDIS 133*.
- Kelly G, Thépaut J-N, 2007. Evaluation of the impact of the space component of the Global Observing System through Observing System Experiments. *In Proceedings of Seminar on recent developments in the use of satellite observations in numerical weather prediction*, ECMWF: Reading, UK. pp 327-348.
- Martinet P, Fourrié N, Guidard V, Rabier F, Montmerle T and Brunel P, 2012. Towards the use of microphysical variables for the assimilation of cloud-affected infrared radiances. *Quart.J.Roy.Meteor.Soc*, *in press*.
- McNally A.P, 2002. A note on the occurrence of cloud in meteorologically sensitive areas and the implications for advanced infrared sounders. *Quart.J.Roy.Meteor.Soc* ,**128**, 2551-2556.
- McNally A.P, 2009. The direct assimilation of cloud-affected satellite infrared radiances in the ECMWF 4D-Var. *Quart.J.Roy.Meteor.Soc*, **135**, 1214-1229.
- Pangaud T, Fourrié N, Guidard V, Dahoui M, Rabier F, 2009. Assimilation of AIRS Radiances affected by Mid-to Low-Level Clouds. *Monthly Weather Review*, **137**, 4276-4292.
- Pavelin E.G, English S.J, Eyre J.R, 2008. The assimilation of cloud-affected infrared satellite radiances for numerical weather prediction. *Quart.J.Roy.Meteor.Soc*, **134**, 737-749.
- Pavelin E.G, Collard A, 2009. NWP SAF Met Office 1D-Var User Manual. NWPSAF-MO-UD-006.
- Rabier, F., Fourrié, N., Chafaï D. and P. Prunet, 2002: Channel selection methods for infrared atmospheric sounding interferometer radiance., *Quart.J.Roy.Meteor.Soc* , **128**, 1011-1027
- Rodgers CD, 2000. Inverse methods for atmospheric soundings: theory and practice. World Scientific: Singapore.
- Seity Y, Brousseau P, Malardel S, Hello G, Benard P, Bouttier F, Lac C, Masson V, 2011. The AROME-France convective-scale operational model. *Monthly Weather Review*, **139**, 976-991.